Off-Design Performance Loss Model for Radial Turbines With Pivoting, Variable-Area Stators

Peter L. Meitner and Arthur J. Glassman

NOVEMBER 1980

NASA

US ARMY
AVRADCOM

NASA
Technical Paper 1708

AVRADCOM
Technical Report 80-C-13

Off-Design Performance Loss Model for Radial Turbines With Pivoting, Variable-Area Stators

Peter L. Meitner
Propulsion Laboratory
AVRADCOM Research and Technology Laboratories
Lewis Research Center
Cleveland, Ohio

Arthur J. Glassman
Lewis Research Center
Cleveland, Ohio

NASA

National Aeronautics
and Space Administration

**Scientific and Technical
Information Branch**

1980

Summary

An off-design performance loss model for a radial turbine with pivoting, variable-area stators was developed through a combination of analytical modeling and analysis of experimental data. A viscous loss model is used for the variation in stator loss with setting angle. Stator vane end-clearance leakage effects are predicted by a proposed clearance-flow model. Rotor loss coefficients were obtained for a turbine rotor previously tested (at constant speed) with six stators having throat areas from 20 to 144 percent of design area. For each of these six configurations, an off-design performance analysis was made to determine the value of rotor loss coefficient that caused the calculated total efficiency at the zero-incidence operating point to match the experimental value. An incidence loss model was selected to obtain best agreement with experimental data.

The rotor loss coefficients were correlated as a function of stator-to-rotor throat area ratio. For area ratios above 0.6, rotor loss coefficient remained constant. As area ratio decreased below 0.5, rotor loss coefficient increased rapidly.

The calculated flows and efficiencies were compared with the experimental data (six stators at design speed over a range of pressure ratio) used to derive the rotor loss coefficients and incidence loss exponents. Overall agreement was very good except for the efficiency variation at 20 percent stator throat area. The same stators had also been tested with versions of the rotor having extended (53 percent throat area) and cutback (137 percent throat area) exducers. The derived loss model was used to calculate turbine performance for these rotors operating with the various stators, and agreement between calculated and experimental values was generally good. This good agreement substantiates the validity of the derived correlation of rotor loss coefficient with stator-to-rotor throat area ratio.

The proposed clearance-flow model predicts increased turbine mass flow and decreased total efficiency as a result of having stator vane end-clearances. These changes become significantly larger with decreasing stator area and vary nearly linearly with clearance.

Introduction

For applications such as helicopter and automotive propulsion, an engine must operate over a wide range of power settings. The radial turbine with a variable-area stator can operate over a broad flow range at nearly constant pressure ratio, temperature, and speed. If this can be accomplished at high efficiency, the turbine can contribute to high engine performance over the entire operating range. However, the stator-area variation as well as the associated vane end-clearances affect turbine performance, and these effects must be known for proper prediction of engine performance.

NASA has developed loss models and computer programs for predicting the design (ref. 1) and off-design (ref. 2) performance of radial turbines. The stator-area-variation and vane end-clearance effects, however, are not included in the loss models used for these programs. Reference 3 presents experimental performance data obtained by testing three rotors having throat areas varying from 53 to 137 percent of design area with six stators having throat areas varying from 20 to 144 percent of design. Separate stator rings with no vane end-clearance were used for these tests; thus these experimental results show the effects of stator area-variation but not the effects of vane end-clearance. This report uses the data of reference 3 in conjunction with analytical modeling to develop an off-design performance loss model for radial turbines with pivoting, variable-area stators.

This report presents the loss model and describes the analysis used to obtain it. Stator losses were varied according to the viscous loss model of reference 1. Rotor loss coefficients were determined by analyzing the experimental data for one rotor operating with the six stators, and these coefficients were correlated as a function of stator-to-rotor throat area ratio. An incidence loss model was selected to obtain the best agreement with the experimental data. Analytical prediction and experimental test results were compared for all three rotors of reference 3 operating with the various stators. A clearance-flow model is proposed to account for the effects of stator vane end-clearance leakage on performance, and sample calculations are presented to show predicted results.

Symbols

A	area, m^2
AR	stator-to-rotor throat area ratio
B	blockage factor at stator exit, ratio of area inside blade passage to area outside blade passage

C	modifier, set equal to 1.0	
c	stator-vane total clearance, m	
$\bar{e}$	kinetic energy loss coefficient	
H	ideal work, J/kg	
h	stator-vane passage height from hub to shroud, m	
i	incidence angle, deg (defined by eq. (19))	
K	rotor loss coefficient	
L	kinetic energy loss, J/kg	
l	surface length, m	
N	rotative speed, rad/sec	
N_s	specific speed, $NQ^{1/2}/H^{3/4}$, dimensionless	
n	incidence exponent	
PR	stator total-pressure ratio (defined by eq. (2))	
p	absolute pressure, N/m^2	
Q	volume flow rate, m^3/sec; or critical velocity ratio function (defined by eq. (7))	
Re	Reynolds number based on stator-vane chord	
r	radius, m	
s	blade spacing at blade-row exit, m	
t	trailing-edge thickness, m	
V	absolute velocity, m/sec	
W	relative velocity, m/sec	
w	mass flow rate, kg/sec	
α	fluid absolute flow angle measured from radial direction at stations 0, 1, 2, and 3 and from axial direction at stations 4 and 5, deg	
β	fluid relative flow angle measured from radial direction at stations 0, 1, 2, and 3 and from axial direction at stations 4 and 5, deg	
γ	ratio of specific heats	
δ	ratio of inlet total pressure to U.S. standard sea-level pressure, $p_{0,t}/p^*$	
ϵ	specific-heat ratio correction, $$\frac{\gamma^*[2/(\gamma^*+1)]^{\gamma^*/(\gamma^*-1)}}{\gamma[2/(\gamma+1)]^{\gamma/(\gamma-1)}}$$	
θ	momentum thickness, m; or squared ratio of critical velocity at inlet to critical velocity at U.S. standard sea-level conditions, $(V_{cr}/V_{cr}^*)^2$	
η	efficiency	
ρ	density, kg/m^3	

Subscripts:

c	clearance
cr	critical
IN	incidence
nc	no clearance
opt	optimum
p	main passage
R	rotor
r	radial component
ref	reference
s	static
t	total
u	tangential component
0	station at turbine inlet
1	station immediately upstream of stator exit
2	station immediately downstream of stator exit
$2D$	two dimensional
3	station immediately upstream of rotor inlet
$3D$	three dimensional
4	station immediately upstream of rotor exit
5	station immediately downstream of rotor exit

Superscript:

$*$	U.S. standard sea-level conditions of 1.013 bars and 288.2 K

Loss-Model Development

A cross section of a typical radial turbine, indicating the flow stations pertinent to the loss-model description, is shown in figure 1. The loss model presented herein is primarily the loss model of reference 2 extended to account for the effects of the stator area-variation as well as the associated vane end-clearance. In addition, the incidence loss model is changed for better agreement with the data. The stator, rotor, and incidence aspects of the loss model are each discussed in the following sections.

Stator Loss

The stator loss model considers the vane-passage flow, the clearance flow, and the mixing process, which also includes the sudden increase in flow area at the trailing edge.
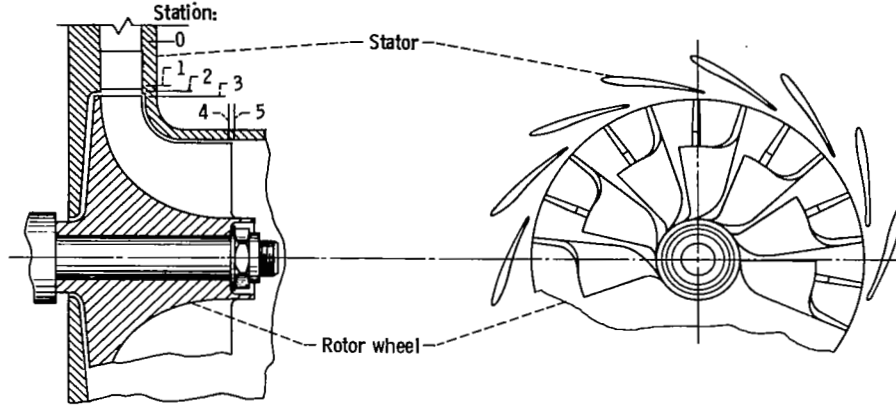
Figure 1. - Cross section of radial turbine.   CD-11857-02

Passage flow.—The stator passage region is defined as the region between the vanes and extending the height $(h-c)$ of the vanes. Since the vane exit angle is known from the turbine design geometry, the vane-passage flow rate is

$$w_p = 2\pi r_1 (h-c) B \rho_1 V_1 \cos \alpha_{1,p} \tag{1}$$

The stator passage loss from station 0 to station 1 is represented by a total-pressure ratio PR that is kept constant for any given stator setting angle over the operating ranges of speed and pressure ratio

$$PR = \frac{p_{1,t}}{p_{0,t}} \tag{2}$$

The change in stator total-pressure ratio with stator angle setting is obtained by expressing the stator pressure ratio in terms of the kinetic energy loss coefficient $\bar{e}_{3D}$

$$PR = \left(\frac{1 - \bar{e}_{3D} - Q_1}{(1 - \bar{e}_{3D})(1 - Q_1)} \right)^{\gamma/(\gamma-1)} \tag{3}$$

and evaluating from the viscous loss equation of reference 1.

$$\bar{e}_{3D} = \frac{EC(\theta_t/l)_{ref}(Re/Re_{ref})^{-0.2}(l/s)\,(A_{3D}/A_{2D})}{\cos \alpha_1 - t/s - HC(\theta_t/l)_{ref}(Re/Re_{ref})^{-0.2}(l/s)} \tag{4}$$

where

$$E = \frac{2\left[(1/1.92)+(Q/3.2)+(Q^2/4.8)+(Q^3/6.72)\right]}{(1/1.68)+(Q/2.88)+(Q^2/4.4)+(Q^3/6.24)} \tag{5}$$

$$H = \frac{(1/1.2)+(3Q/1.6)+(5Q^2/2.0)+(7Q^3/2.4)+(9Q^4/2.8)}{(1/1.68)+(Q/2.88)+(Q^2/4.4)+(Q^3/6.24)} \tag{6}$$

$$Q = \left(\frac{\gamma-1}{\gamma+1}\right)\left(\frac{V}{V_{cr}}\right)^2 \tag{7}$$

$$\left(\frac{\theta_t}{l\,Re^{-0.2}}\right)_{ref} = 0.03734 \tag{8}$$

3

The three-dimensional kinetic energy loss coefficient $\bar{e}_{3D}$ accounts for the profile and end-wall viscous losses. For a given value of V/V_{cr}, the major effect of varying the stator angle setting is the change in flow area, which is represented primarily by the cosine term in the denominator of equation (3). Equations (3) to (7) are evaluated at the design value of V/V_{cr}, which is 0.618 for the stator of reference 3. For the design-rotor turbine of reference 3, closing the stator vanes from 144 percent of design area (stator exit angle of 64.7°) to 20 percent of design area (85.0°) resulted in the stator total-pressure ratio decreasing from 0.9902 to 0.9445.

Clearance flow.—In the absence of available experimental data, a clearance-flow model is proposed to account for stator end-clearance leakage. A clearance-flow region is defined as that region extending from the ends of the stator vane to the passage end walls (hub or tip end). It is the area unblocked by vanes and extending over the clearance height c. This clearance-flow model results in increased flow and decreased work, consistent with the experimental results of reference 4 for an axial turbine with pivoted stator vanes, and is based on the following assumptions:

(1) The clearance flow expands to the same stator-exit static pressure as the vane-passage flow.

(2) The clearance flow has the same total-pressure loss as the vane-passage flow.

(3) Stator-inlet moment of tangential momentum is conserved in the clearance flow.

From these assumptions, the velocities and densities must be the same for both flows. Only the flow angle will differ. The clearance-flow exit angle is determined from the conservation of moment of tangential momentum.

$$r_1 V_{u,1,c} = r_1 V_1 \sin \alpha_{1,c} = (rV_u)_0 \tag{9}$$

$$\alpha_{1,c} = \sin^{-1} \left[\frac{(rV_u)_0}{(rV)_1} \right] \tag{10}$$

Thus the clearance flow rate is

$$w_c = 2\pi r_1 c \rho_1 V_1 \cos \alpha_{1,c} \tag{11}$$

Mixing.—The mixing process that takes place between stations 1 and 2, which are assumed to be at the same radius, includes the mixing of the passage and clearance flows, as well as the expansion of the mixed flow as it fills the space behind the vane trailing edges. The expansion behind the trailing

edges takes place even with no clearance flow. Mixing is assumed to occur at constant static pressure with tangential momentum being conserved.

For the mixing process, the total flow is the sum of the passage and clearance flows

$$w = w_p + w_c$$

$$= 2\pi r_1 \rho_1 V_1 \left[(h-c)B \cos \alpha_{1,p} + c \cos \alpha_{1,c} \right] \tag{12}$$

Conservation of tangential momentum between stations 1 and 2 yields

$$V_{u,2} = \frac{w_p}{w} V_{u,1,p} + \frac{w_c}{w} V_{u,1,c} \tag{13}$$

or

$$V_{u,2} = \frac{V_1}{w} (w_p \sin \alpha_{1,p} + w_c \sin \alpha_{1,c}) \tag{14}$$

The continuity equation

$$\rho_2 V_{r,2} = \frac{w}{2\pi r_2 h} \tag{15}$$

is solved iteratively with equation (14) for $V_{r,2}$ to complete definition of the mixed flow at station 2. As in reference 2, the station 3 conditions are obtained from the station 2 conditions by assuming no loss (constant total pressure) and conservation of moment of tangential momentum.

The predicted effects of end clearance on performance can be seen from equations (12) and (14). The clearance flow angle will generally be much less than the passage flow angle. Therefore increased clearance will result in increased flow rate and decreased tangential velocity, which yields decreased work.

Rotor Loss

In the loss model of reference 2, the rotor loss is calculated by

$$L_R = K \left(\frac{W_3^2 \cos^2 i_3 + W_4^2}{2} \right) \tag{16}$$

where the rotor loss coefficient K is maintained constant over the operating ranges of pressure ratio and speed. The rotor loss L_R represents all losses in the rotor except incidence loss. This includes the three-dimensional viscous loss, the disk friction loss on the back face of the rotor, the loss due to clearance between the rotor and the outer casing, and the wake mixing loss. A variation in rotor loss coefficient with stator area is expected because of changes in rotor reaction. In this report, such a variation is obtained by using the off-design performance computer program of reference 2 to determine the values of rotor loss coefficient that caused the calculated total efficiency to match the test data of reference 3.

In reference 3, a design rotor and two modified rotors (fig. 2)—one with the exducer extended to reduce rotor exit area to 53 percent of design area and one with the exducer cut back to increase rotor exit area to 137 percent of design area—were tested with stators having throat areas of 144, 125, 100, 66, 42, and 20 percent of the design value. All stators were fixed and thus had no vane end-clearance leakage. All configurations used the same vane profile, but each used a different number of vanes and setting angles to achieve the desired flow areas. The number of vanes and angles for each configuration are shown in table I. All tests were conducted at equivalent design speed over a range of pressure ratios. The data for the design rotor were used to determine the variation in rotor loss coefficient with stator area. The data for the extended and cutback rotors were used to test the developed correlation.
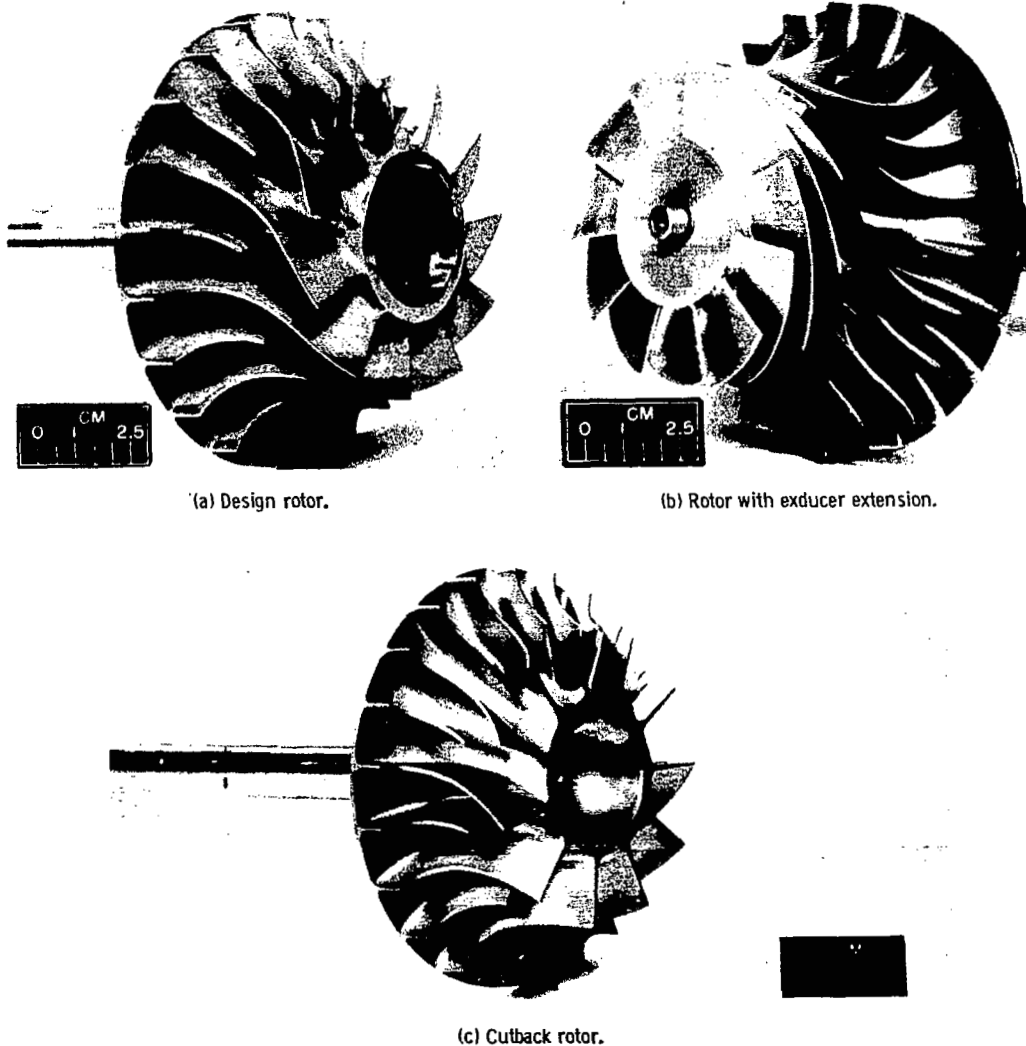

(a) Design rotor.

(b) Rotor with exducer extension.

(c) Cutback rotor.

Figure 2. - Rotor configurations.

TABLE I. – SUMMARY OF GEOMETRIC DATA AND

LOSS COEFFICIENTS FOR DESIGN, EXTENDED,

AND CUTBACK ROTOR CONFIGURATIONS

(a) Design rotor configurations. Rotor-exit flow angle, β_4, -56.86°.

Stator throat area, percent of design	Number of stator vanes	Stator-exit flow angle, α_1, deg	Stator total-pressure ratio, PR	Rotor loss coefficient, K
144	13	64.70	0.9902	0.180
125	13	68.00	.9880	.180
100	13	72.47	.9866	.220
66	15	77.75	.9823	.410
42	17	81.38	.9702	1.200
20	17	85.00	.9447	9.250

(b) Extended rotor configurations. Rotor-exit flow angle, β_4, -72.56°.

100	13	72.47	0.9927	0.180
66	15	77.75	.9854	.180
42	17	81.38	.9699	.280
20	17	85.00	.9450	4.250

(c) Cutback rotor configurations. Rotor-exit flow angle, β_4, -42.07°.

144	13	64.70	0.9882	0.210
125	13	68.00	.9878	.250
100	13	72.47	.9864	.360

For each stator tested with the design rotor, turbine efficiency at zero incidence angle (with respect to the optimum rotor-inlet flow angle) was calculated by the computer program of reference 2 over a range of rotor loss coefficient values. These results are presented in figure 3. Indicated on each curve is the zero-incidence value of experimental total efficiency. The loss coefficients associated with the marked points in figure 3 are divided by the lowest value (0.18 for both 144 and 125 percent stator throat area) and plotted against stator-to-rotor throat area ratio, which is selected as the correlating parameter because it reflects turbine reaction and can be evaluated directly from turbine geometry. This generalized relationship, as shown in figure 4, yields a smooth correlation curve. The stator-to-rotor area ratio AR is defined by

$$AR = \frac{A_1 \cos \alpha_1}{A_4 \cos \beta_4} \qquad (17)$$

As shown in figure 4, the rotor loss coefficient remains constant for area ratios above about 0.6. As area ratio decreases below 0.5, the rotor loss coefficient increases rapidly. This trend appears to be consistent with calculated rotor flow characteristics. Shown in figure 5 for the six stator areas are the design rotor-hub loading diagrams reproduced from reference 3. For stator areas of 100 percent (about 0.5 stator-to-rotor exit area ratio) and larger, all velocities are positive and the free-stream velocity levels indicate a significant acceleration across the rotor. As stator area decreases below 100 percent, areas of negative velocity (implying separation) become larger and rotor overall flow acceleration rapidly decreases. At 42 percent area there is an
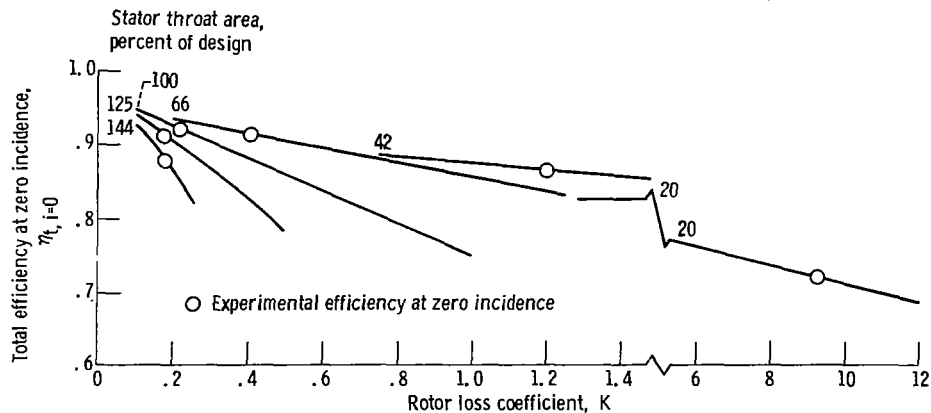

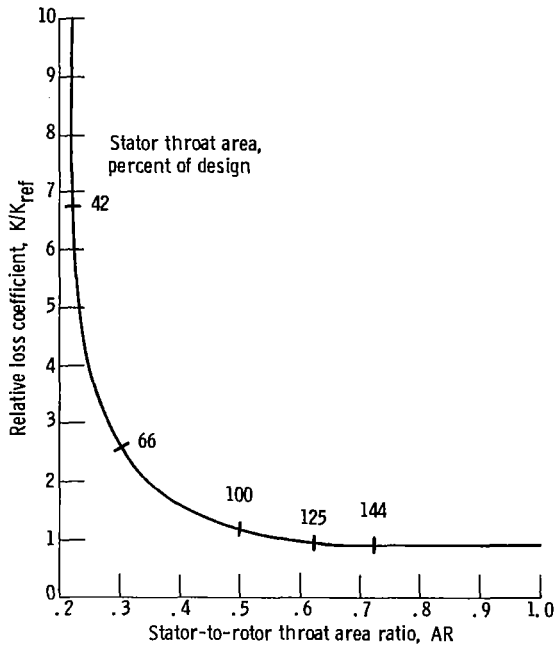Figure 3. – Total efficiency as function of rotor loss coefficient – design rotor.

Figure 4. - Rotor relative loss coefficient as function of stator-to-rotor throat area ratio.

overall deceleration; at 20 percent area the entire rotor hub exit flow is calculated to be negative.

Incidence Loss

In the loss model of reference 2, the incidence loss was expressed as

$$L_{IN} = \frac{W_3^2 \sin^n i_3}{2} \tag{18}$$

where the exponent n was determined to be 2 for negative incidence and 3 for positive incidence. The incidence angle is defined with reference to the optimum rotor-inlet flow angle as

$$i_3 = \beta_3 - \beta_{3,opt} \tag{19}$$

During this analysis it became evident that the foregoing loss equation was not entirely consistent with the reference 3 data in the region of negative incidence. Examination of the experimental

(a) 20 percent stator throat area.

(b) 42 percent stator throat area.

(c) 66 percent stator throat area.

(d) 100 percent stator throat area.

(e) 125 percent stator throat area.

(f) 144 percent stator throat area.
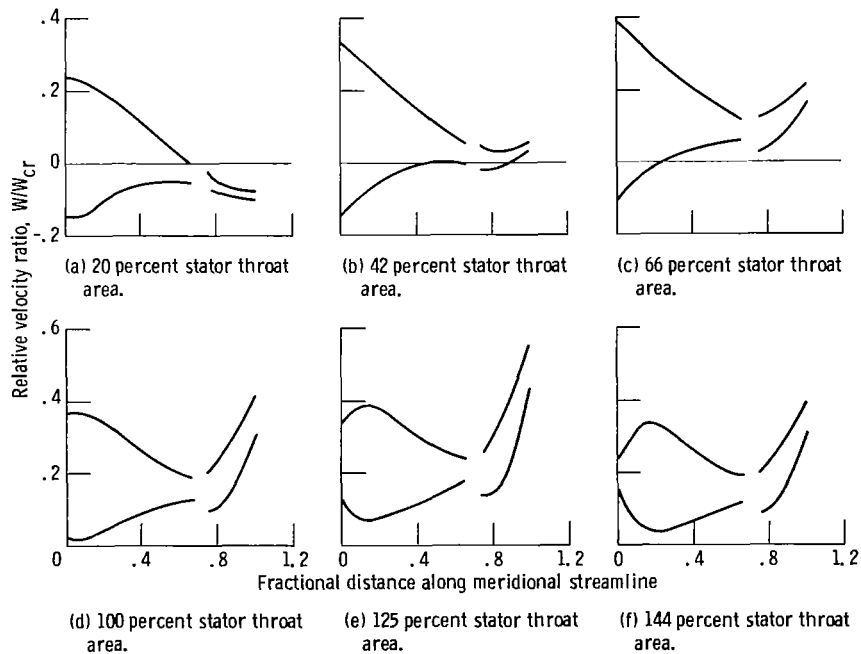
Figure 5. - Blade surface velocities at equivalent design speed and pressure ratio - design-rotor hub section. (From ref. 3.)

7

performance maps (shown in ref. 2) used to derive the incidence loss exponents showed very limited data in the negative incidence region. Those data were therefore not very definitive for purposes of modeling the negative incidence loss.

The experimental results (ref. 3) being analyzed herein provided a much better data base, both in amount of data and range of incidence angle, for modeling incidence loss. To obtain a continuous variation in incidence loss with exponent n at negative incidence angles, the equation for incidence loss used herein was changed to that used in reference 5.

$$L_{IN} = \frac{W_3^2(1 - \cos^n i_3)}{2} \tag{20}$$

The effect of the incidence exponent n on calculated efficiency is shown in figure 6. The best overall match between analysis and experiment, based on all six stators with the design rotor, was obtained with an exponent n of 2.5 for negative incidence and 1.75 for positive incidence. This result is different from results for axial turbines, where losses at positive incidence are usually more severe (higher exponent) than losses at comparable negative incidence (ref. 5). This difference is probably due to the very large slip angles for radial turbines. The modified incidence loss model provided as good an analytical match of the reference 2 data base as did the original incidence model.

Loss-Model Evaluation

In this section, turbine overall performance calculated by using the developed loss model is compared with the experimental performance data from the design rotor and the modified rotors of reference 3. Also, the effects of stator vane end-clearance as calculated by the loss model are presented.
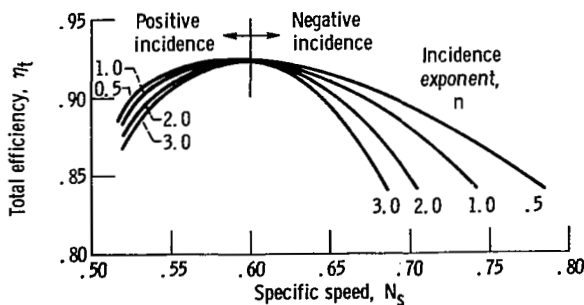
Figure 6. - Calculated total efficiency as function of incidence exponent and specific speed - design stator and rotor.

Design Rotor

The experimental data for the design rotor with the six stators (144, 125, 100, 66, 42, and 20 percent design throat area) were used as the data base for the variation in rotor loss coefficient with stator area, as well as for the modified incidence loss model. Figures 7, 8, and 9 present the overall comparisons between calculated and experimental mass flow rate, total efficiency, and static efficiency, respectively, at constant design speed. The zero-incidence match points are indicated in figure 8. Overall agreement between analysis and experiment is good to excellent, with the exception of the 20-percent-area case. This demonstrates the applicability of the incidence loss model over a wide range of incidence angle, which varied from about -40° to 90° for these data. For 20 percent stator area, the indicated extensive flow separation (fig. 5) would cause the actual flow angle at the rotor exit to deviate substantially from the
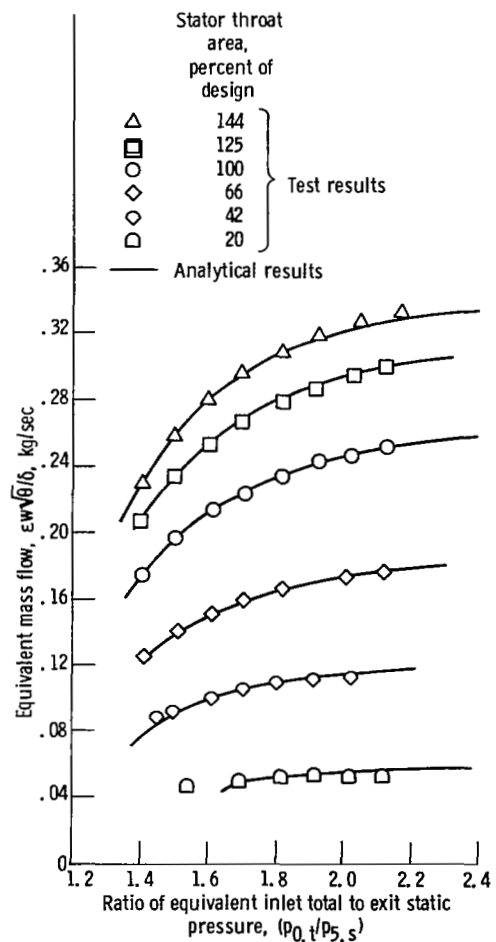
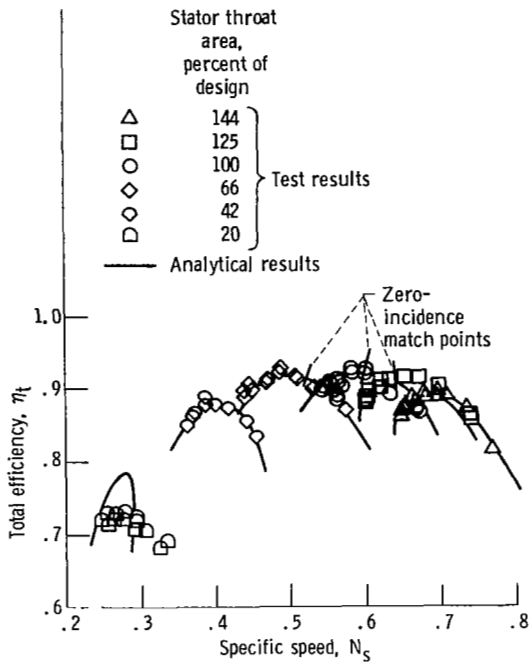Figure 7. - Design-rotor mass flow as function of pressure ratio.

Figure 8. - Turbine total efficiency as function of specific speed - design rotor.
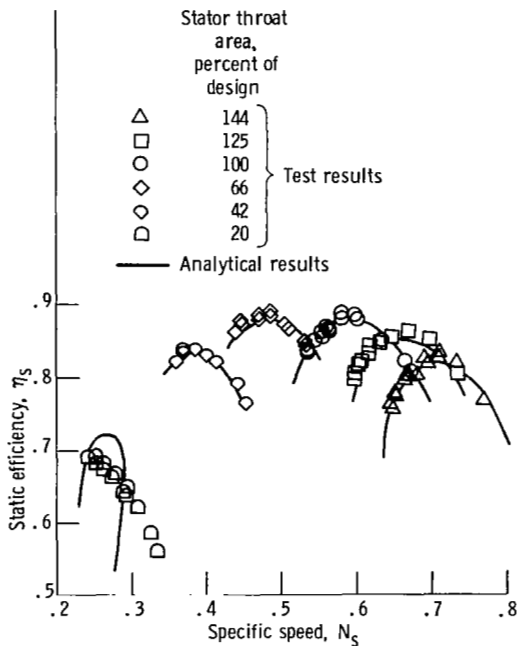

Figure 9. - Turbine static efficiency as function of specific speed - design rotor.

rotor-exit blade angle and would thus result in the analysis not matching the experimental trend of the efficiency data.

Modified Rotors

The experimental tests of reference 3 were also conducted with a cutback rotor exducer and an extended rotor exducer having throat areas of 137 and 53 percent, respectively, of the design rotor area. The cutback rotor was - tested with stators corresponding to 144, 125, and 100 percent of the design-stator throat area, and the extended rotor was tested with stators corresponding to 100, 66, 42, and 20 percent of the design-stator throat area.

The developed loss model was used to predict the results of the cutback- and extended-rotor tests. The loss coefficients used for the prediction are shown in table I. They were obtained from figure 4. Figures 10, 11, and 12 show equivalent mass flow, total efficiency, and static efficiency, respectively, for the cutback rotor. Figures 13, 14, and 15 show the same information for the extended rotor. In general the agreement between experiment and analysis is satisfactory to excellent with regard to both level and trend. For the same reasons as discussed for the design rotor, the experimental and analytical
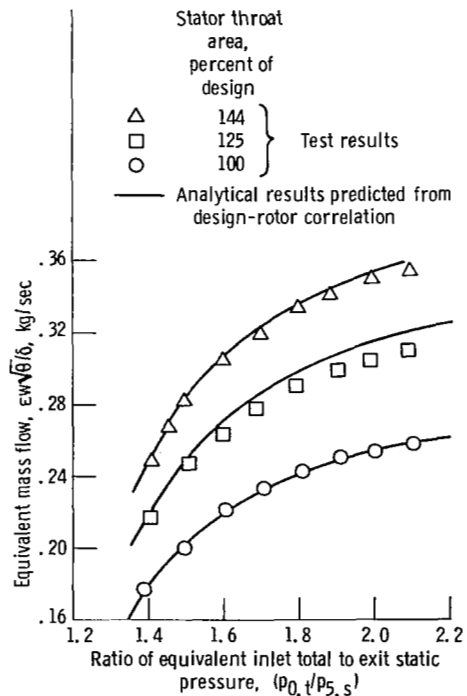

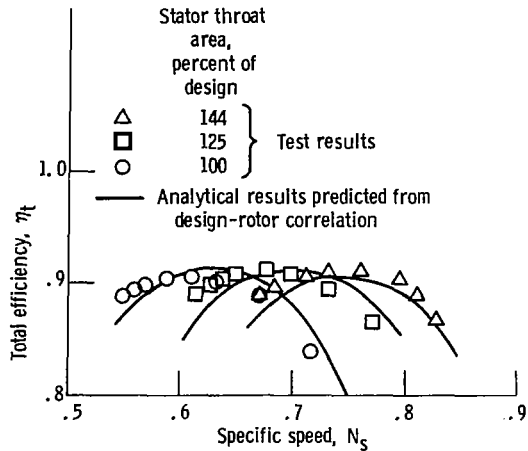Figure 10. - Mass flow as function of pressure ratio - cutback rotor.

Figure 11. - Turbine total efficiency as function of specific speed - cutback rotor.
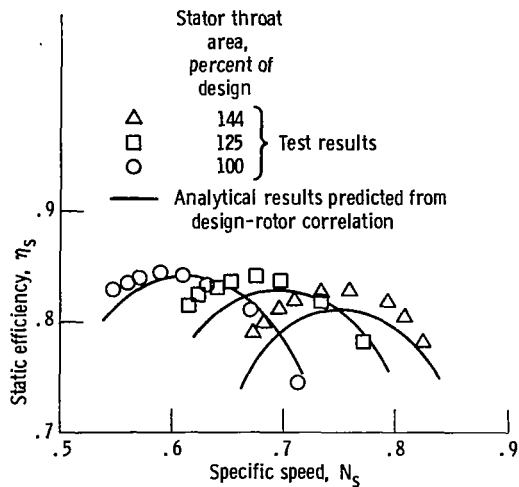

Figure 12. - Turbine static efficiency as function of specific speed - cutback rotor.
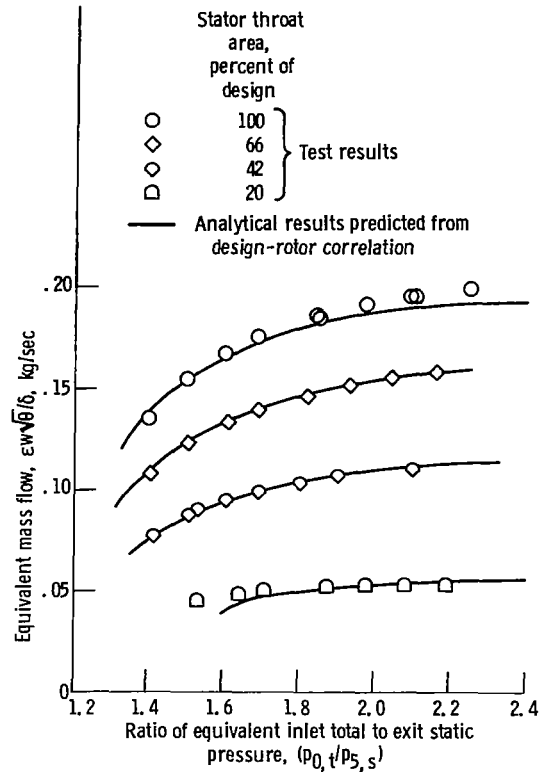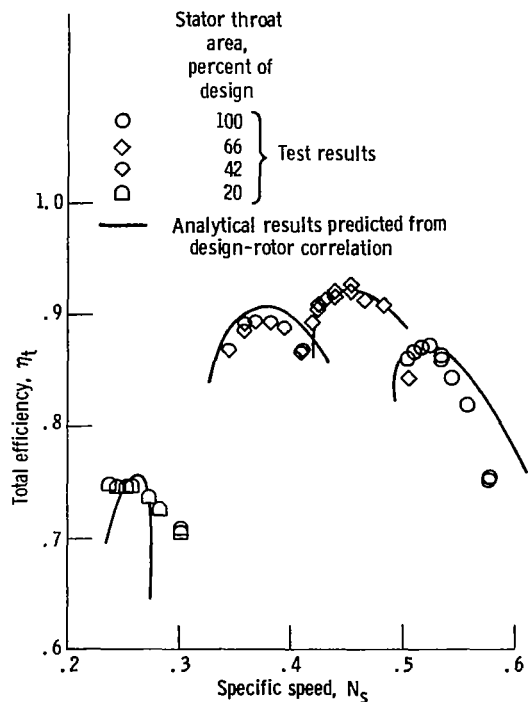

Figure 13. - Mass flow as function of pressure ratio - extended rotor.

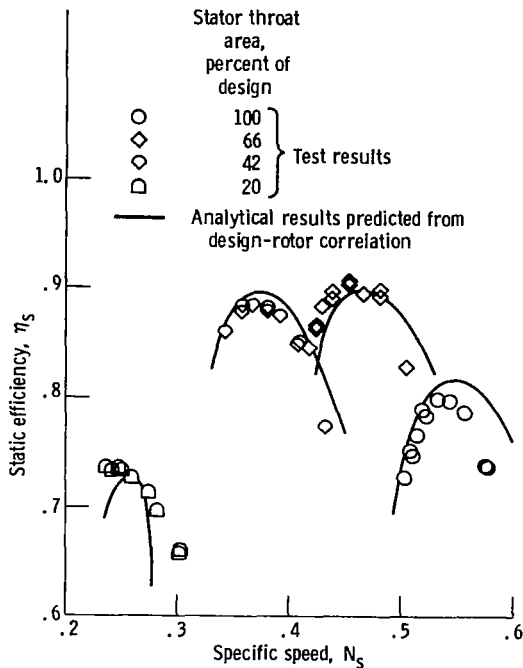Figure 14. - Turbine total efficiency as function of specific speed - extended rotor.

efficiency trends for the 20 percent stator area do not match as well as those for the other stators. The overall good agreement for the extended and cutback rotors substantiates the validity of the derived correlation of rotor loss coefficient with stator-to-rotor throat area ratio.

Stator Clearance

All data of reference 3 were taken with fixed stators having no vane end-clearance, and a direct comparison between analytical and experimental results for stator vane end-clearance leakage is thus not possible. The described clearance-flow model was used to predict turbine performance for the

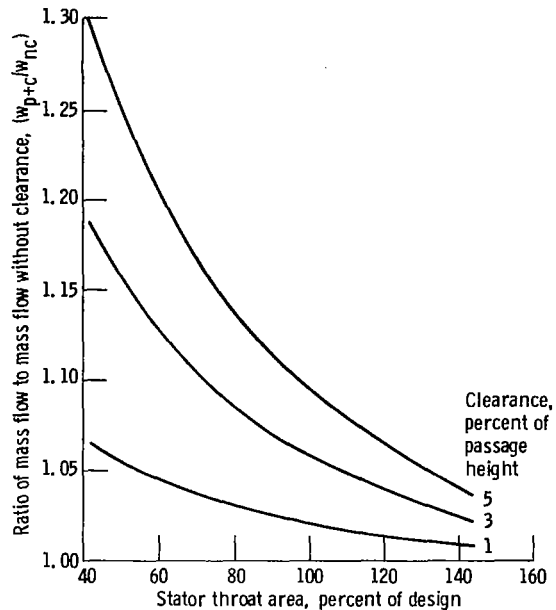Figure 15. – Turbine static efficiency as function of specific speed – extended rotor.

Figure 16. – Mass flow as function of stator throat area and clearance – design rotor at constant pressure ratio.

design rotor with various stator vane end-clearances. For all calculations with stator vane end-clearance, the stator total-pressure ratio PR and the rotor loss coefficient K were assumed to be equal to the no-clearance values.

The calculated effect of stator vane end-clearance on mass flow at a constant turbine pressure ratio over a range of stator areas is shown in figure 16. These results are independent of turbine pressure ratio. For a given stator clearance, the mass flow ratio increases rapidly with decreasing stator area. This occurs because the clearance flow becomes a larger portion of the total flow as the passage area decreases. As stator clearance is increased at a fixed stator area, the mass flow increases at a rate nearly linear with clearance.

The calculated effect of stator clearance on total efficiency at constant turbine pressure ratio over a range of stator areas is shown in figure 17. These results vary only slightly with turbine pressure ratio. For a given stator clearance, the efficiency penalty due to the clearance flow becomes significantly larger as stator area decreases. This occurs primarily as a result of the greater loss in tangential momentum as clearance flow becomes a larger part of the total flow. As stator clearance is increased at a fixed stator area, the efficiency penalty increases at a rate nearly linear with clearance.
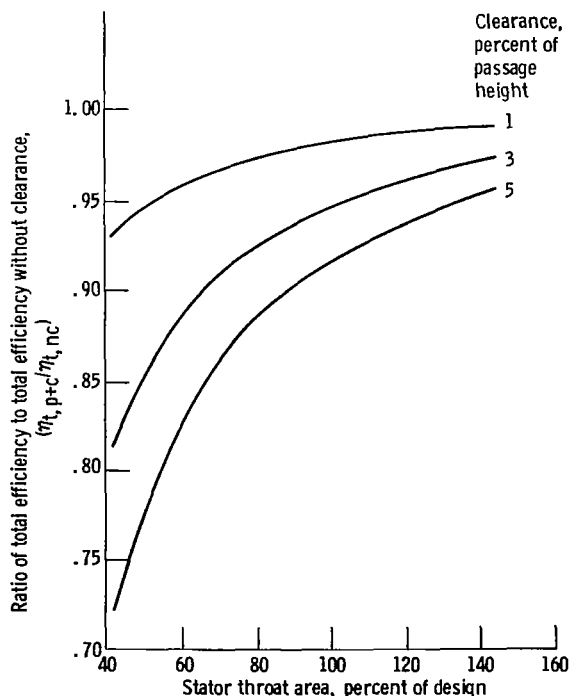

Figure 17. – Total efficiency as function of stator throat area and clearance – design rotor at constant pressure ratio.

11

Summary of Results

An off-design performance loss model for a radial turbine with pivoting, variable-area stators was developed through a combination of analytical modeling and analysis of experimental data. A viscous loss model is used for the variation in stator loss with setting angle. Stator vane end-clearance leakage effects are predicted by a clearance-flow model. Rotor loss coefficients were obtained for a turbine rotor previously tested (at constant speed) with six stators having throat areas from 20 to 144 percent of design area. For each of these six configurations, an off-design performance analysis was made to determine the value of rotor loss coefficient that caused the calculated total efficiency of the zero-incidence operating point to match the experimental value. An incidence loss model was selected to obtain best agreement with experimental data. The predicted turbine performance is compared with experimental results for the design rotor as well as for versions of the rotor having extended and cutback exducers. Sample calculations were made to show the effects of stator vane end-clearance leakage. The major results of these analyses are as follows:

1. The six rotor loss coefficients obtained by analysis from the experimental data provided a smooth curve when plotted against stator-to-rotor throat area ratio. For area ratios above 0.6, rotor loss coefficient remained constant. As area ratio decreased below 0.5, rotor loss coefficient increased rapidly. This variation in rotor loss coefficient is consistent with calculated rotor internal flow characteristics.

2. Comparison of the calculated flows and efficiencies with the experimental data (i.e., data for the design rotor) used to derive the rotor and incidence loss coefficients showed very good overall agreement except for the efficiency variation at 20 percent stator throat area. This good overall agreement demonstrates the applicability of the incidence model over a wide incidence range, in this case from about -40° to 90°. For the 20 percent stator throat area, where analysis indicated extensive rotor flow separation, the calculated efficiency trend did not match the experimental data.

3. Comparison of calculated flows and efficiencies for the extended exducer (53 percent throat area) and cutback exducer (137 percent throat area) versions of the rotor showed generally good agreement except, again, for the 20 percent stator area. This good agreement substantiates the validity of the derived correlation of rotor loss coefficient with stator-to-rotor throat area ratio.

4. The stator vane end-clearance leakage model predicts increasing mass flow and decreasing efficiency as a result of vane end-clearances. These changes become significantly larger with decreasing stator area and vary almost linearly with clearance.

References

1. Glassman, Arthur J.: Computer Program for Design Analysis of Radial-Inflow Turbines. NASA TN D-8164, 1976.

2. Wasserbauer, Charles A.; and Glassman, Arthur J.: FORTRAN Program for Predicting Off-Design Performance of Radial-Inflow Turbines. NASA TN D-8063, 1975.

3. Kofskey, Milton G.; and Nusbaum, William J.: Effects of Specific Speed on Experimental Performance of a Radial-Inflow Turbine. NASA TN D-6605, 1972.

4. Kofskey, Milton G.; and McLallin, Kerry L.: Cold-Air Performance of Free Power Turbine Designed for 112-Kilowatt Automotive Gas-Turbine Engine. Vol. 3: Effect of Stator Vane End Clearances on Performance. DOE/NASA/1011-78/29. NASA TM-78956, 1978.

5. Roelke, Richard J.: Miscellaneous Losses. Turbine Design and Application, Vol. 2, Arthur J. Glassman, ed., NASA SP-290 Vol. 2, 1973, pp. 125-148.

1. Report No. NASA TP-1708 AVRADCOM TR-80-C-13	2. Government Accession No.	3. Recipient's Catalog No.
4. Title and Subtitle OFF-DESIGN PERFORMANCE LOSS MODEL FOR RADIAL TURBINES WITH PIVOTING, VARIABLE-AREA STATORS		5. Report Date November 1980
		6. Performing Organization Code
7. Author(s) Peter L. Meitner and Arthur J. Glassman		8. Performing Organization Report No. E-455
		10. Work Unit No. 505-32
9. Performing Organization Name and Address NASA Lewis Research Center and Propulsion Laboratory AVRADCOM Research and Technology Laboratories Cleveland, OH 44135		11. Contract or Grant No.
		13. Type of Report and Period Covered Technical Paper
12. Sponsoring Agency Name and Address National Aeronautics and Space Administration Washington, DC 20546 and U.S. Army Aviation Research and Development Command St. Louis, MO 63166		14. Sponsoring Agency Code

15. Supplementary Notes

Peter L. Meitner: Propulsion Laboratory, AVRADCOM Research and Technology Laboratories.
Arthur J. Glassman: Lewis Research Center.

16. Abstract

An off-design performance loss model was developed for variable-stator (pivoted vane), radial turbines through analytical modeling and experimental data analysis. Stator loss is determined by a viscous loss model; and stator vane end-clearance leakage effects are determined by a clearance-flow model. Rotor loss coefficients were obtained by analyzing the experimental data from a turbine rotor previously tested with six stators having throat areas from 20 to 144 percent of design area and were correlated with stator-to-rotor throat area ratio. An incidence loss model was selected to obtain best agreement with experimental results. Predicted turbine performance is compared with experimental results for the design rotor as well as with results for extended and cutback versions of the rotor. Sample calculations were made to show the effects of stator vane end-clearance leakage.

17. Key Words (Suggested by Author(s)) Radial turbine Turbine loss model Variable geometry	18. Distribution Statement Unclassified – Unlimited Subject Category 07
19. Security Classif. (of this report) Unclassified	20. Security Classif. (of this page) Unclassified	21. No. of Pages 14	22. Price* A02

National Aeronautics and
Space Administration

Washington, D.C.
20546

SPECIAL FOURTH CLASS MAIL
BOOK

U.S.MAIL

```
  8    1 1U,A,         103180 S00903DS
DEPT OF THE AIR FORCE
AF WEAPONS LABORATORY
ATTN: TECHNICAL LIBRARY (SUL)
KIRTLAND AFB NM 87117
```
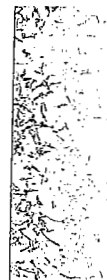
NASA

POSTMASTER: If Undeliverable (Section 158
Postal Manual) Do Not Return